

DIFFRACTIVE AND EXCLUSIVE MEASUREMENTS AT CDF*

MICHELE GALLINARO[†]

*Laboratory of Experimental High Energy Physics
The Rockefeller University
1230 York Avenue, New York, NY 10021, USA*

Experimental results from the CDF experiment at the Tevatron in $p\bar{p}$ collisions at $\sqrt{s}=1.96$ TeV are presented on the diffractive structure function at different values of the exchanged momentum transfer squared in the range $0 < Q^2 < 10,000$ GeV², on the four-momentum transfer $|t|$ distribution in the region $0 < |t| < 1$ GeV² for both soft and hard diffractive events up to $Q^2 \approx 4,500$ GeV², and on the first experimental evidence of exclusive production in both dijet and diphoton events. A novel technique to align the Roman Pot detectors is also presented.

1. Quantum Chromodynamics and diffraction

Diffractive processes are characterized by a final state in which a large region of rapidity is not filled with particles (“rapidity gap”) and where the incident hadrons that survive are emitted at small angles with respect to the original beam direction. The traditional “pomeron” can be defined within the framework of Quantum Chromodynamics (QCD) and can be described as a composite entity of quarks and gluons¹. The goal of the CDF diffractive studies is two-fold: (a) to obtain results which can help decipher the QCD nature of the Pomeron, such as the measurement of the diffractive structure function (DSF) and $|t|$ distributions, and (b) to measure exclusive production rates (dijet, χ^0 , $\gamma\gamma$), which could be used to establish benchmark calibrations for exclusive Higgs production at the Large Hadron Collider (LHC) experiments². At CDF, the study of diffractive events has been performed by tagging events with either a rapidity gap or a leading hadron.

*Presented at the “XIV International Workshop on Deep Inelastic Scattering” (DIS2006), Tsukuba, Japan, 20-24 April, 2006

[†]Representing the CDF collaboration.

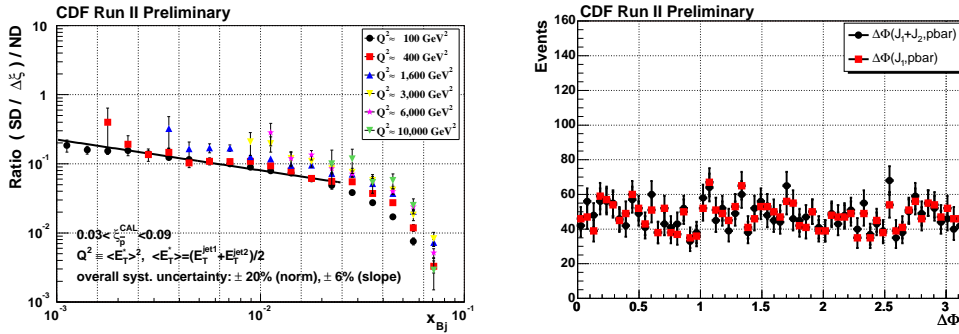


Figure 1. *Left:* Ratio of diffractive to non-diffractive dijet event rates as a function of x_{Bj} (momentum fraction of struck parton in the antiproton) for different values of $E_T^2 \equiv Q^2$; *Right:* Azimuthal angle difference between the jets and the outgoing antiproton in the RP+J5 sample. The jet angle is that of the leading jet (red squares) or the average of the angles of the two leading jets (black circles).

2. Diffractive structure functions

The gluon and quark content of the interacting partons can be investigated by comparing single diffractive (SD) and non-diffractive (ND) events. SD events are triggered on a leading antiproton in the Roman Pot Spectrometer (RPS)³ and at least one jet, while the ND trigger requires only a jet in the calorimeters. The ratio of SD to ND dijet production rates (N_{jj}) is proportional to the ratio of the corresponding structure functions (F_{jj}), $R_{\frac{SD}{ND}}(x, \xi, t) = \frac{N_{jj}^{SD}(x, Q^2, \xi, t)}{N_{jj}(x, Q^2)} \approx \frac{F_{jj}^{SD}(x, Q^2, \xi, t)}{F_{jj}(x, Q^2)}$, and can be measured as a function of the Bjorken scaling variable $x \equiv x_{Bj}$ ⁴. In the ratio, jet energy corrections approximately cancel out, thus avoiding dependence on Monte Carlo (MC) simulation. Results are consistent with those of Run I⁵, hence confirming a breakdown of factorization. In Run II, the jet E_T spectrum extends to $E_T^{\text{jet}} \approx 100 \text{ GeV}$. Preliminary results indicate that the ratio does not strongly depend on $E_T^2 \equiv Q^2$ in the range $100 < Q^2 < 10,000 \text{ GeV}^2$ (Fig. 1, left). The relative normalization uncertainty cancels out in the ratio, and the results indicate that the Q^2 evolution, mostly sensitive to the gluon density, is similar for the proton and the pomeron.

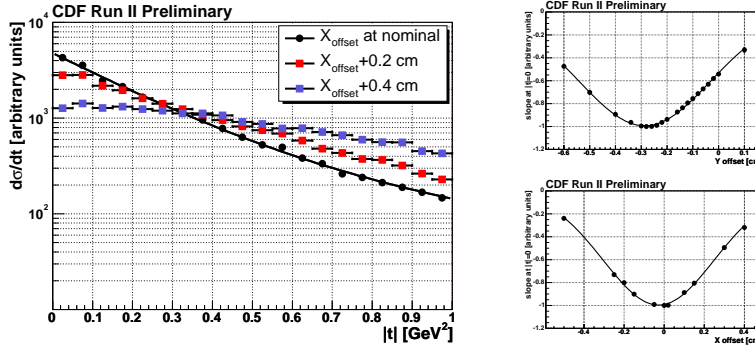


Figure 2. *Left:* t -distribution of reconstructed RPS tracks for positive X_{offset} shifts; *Right:* $|b|$ slope versus Y (top) and X (bottom) offsets.

3. Measurement of $|t|$ distributions

3.1. Dynamic alignment of Roman Pot detectors

The antiproton fractional momentum loss, ξ , and four-momentum transfer squared, t , of SD events can be determined from tracks reconstructed in the RPS and the position of the event vertex at the Interaction Point (IP) using the beam transport matrix between the IP and RPS. Crucial for this measurement is the determination of the detector alignment with respect to the beam. The RPS detectors can be aligned by seeking a maximum of the $d\sigma/dt$ distribution at $t = 0$ for SD events (Fig. 2, left). Offsets in both the X and Y coordinates of the RPS detectors with respect to the beam are adjusted until a maximum for $|d\sigma/dt|$ is found at $t = 0$, when the RPS fiber tracker is correctly aligned with respect to the beam (Fig. 2, right). This innovative method is very precise and quite general, and can be used to accurately calibrate the RPS detector position with respect to the beam in CDF using current data or in future experiments at the LHC. The accuracy of the RPS alignment calibration at CDF is $\Delta X \approx \pm 30 \mu\text{m}$ and $\Delta Y \approx \pm 30 \mu\text{m}$, respectively.

3.2. $|t|$ distributions

SD events studied contain both soft and hard diffractive interactions. An exponential fit with a slope b and arbitrary normalization agrees well with the data in the region $0 < |t| < 1 \text{ GeV}^2$ for different data samples in which the mean dijet transverse energy is increasingly larger (Fig. 3, left). The

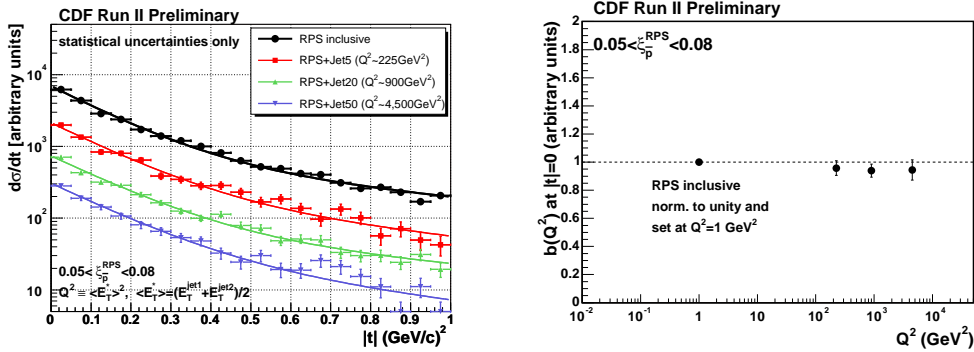


Figure 3. *Left:* $|t|$ -distribution measurement for soft and hard SD events; *Right:* b -slope at different Q^2 values (slope of RPS inclusive data is normalized to $b = 1$).

measured $|t|$ distribution does not show diffractive minima or ‘‘dips’’, which could have been caused by the interference terms of imaginary and real parts of the interacting partons. When comparing soft and hard diffractive events, results show that the b parameter is equal within uncertainties up to $Q^2 \approx 4,500 \text{ GeV}^2$ (Fig. 3, right).

The azimuthal angle difference, $\Delta\Phi$, between the jets and the outgoing antiproton is a flat distribution shown in Figure 1 (right), and it does not show any correlation.

4. Exclusive dijet production

Exclusive production at the Tevatron can be used as a benchmark to establish predictions on exclusive diffractive Higgs production, a process with a much smaller cross section⁶. This is the case in Higgs production through the Double Pomeron Exchange (DPE) processes $p\bar{p} \rightarrow pH\bar{p}$ (or $pp \rightarrow pHp$), where the leading hadrons in the final state are produced at small angles with respect to the direction of the incoming particles and two large forward rapidity gap regions are present on opposite sides of the interaction. The Higgs production process through $gg \rightarrow H$ is replaced by the $gg \rightarrow$ jet jet process, with a much larger production cross section. The characteristic signature of this type of events is a leading nucleon and/or a rapidity gap on both forward regions, and it results in an exclusive dijet final state produced together with both the leading proton and anti-proton surviving the interaction and escaping in the very forward region. The CDF RPS spectrometer can tag the anti-proton, while the proton is inferred by the

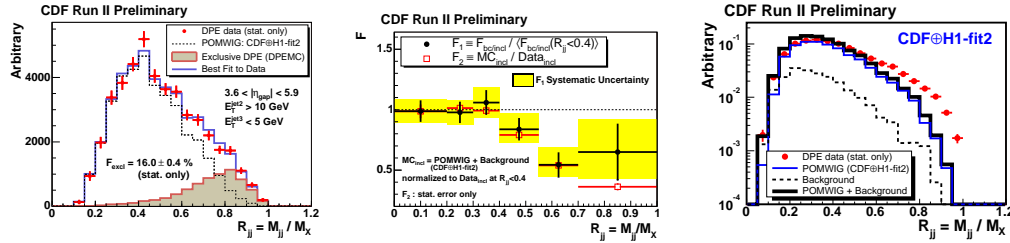


Figure 4. *Left:* dijet mass fraction in DPE data (points) and best fit (solid) obtained from POMWIG MC events (dashed) and exclusive dijet MC events (shaded); *Center:* normalized ratio of heavy flavor jets to all jets as a function of dijet mass fraction. *Right:* R_{jj} distribution for the data (points) and POMWIG MC prediction (thick histogram), composed of DPE dijet events (thin) and non-DPE events (dashed). Data and MC are normalized to the same area.

presence of an adjacent large ($\Delta\eta > 3$) rapidity gap. The dijet mass fraction (R_{jj}), defined as the dijet invariant mass (M_{jj}) divided by the mass of the entire system, $M_X = \sqrt{\xi_p \cdot \xi_p \cdot s}$, is calculated using all available energy in the calorimeter. If jets are produced exclusively, R_{jj} should be equal to one. Owing to hadronization effects, underlying event energy spilling out of the jet reconstruction cone, and radiation from the jets, the sharp peak from exclusive production is smeared out to a wider distribution. The search is performed by comparing data with MC expectations. At large R_{jj} values, the excess of events in the data with respect to inclusive DPE dijet production, which is described by POMWIG⁷ MC, is well accounted for by the DPEMC⁸ (or equivalently ExHuME⁹) MC sample of exclusive events (Fig. 4, left).

The quark/gluon composition of dijet final states can be used to provide additional information on exclusive dijet production. At leading order (LO) $gg \rightarrow gg$ process is dominant while $gg \rightarrow q\bar{q}$ is strongly suppressed. This “suppression” mechanism can be used to improve the sensitivity to exclusive production. Thanks to high tagging efficiency of heavy flavor jets and low mistag rate, b/c -quarks are selected. The ratio ($F_{bc/\text{incl}}$) of heavy flavor tagged jets divided by all inclusive jet events is measured as a function of R_{jj} and is normalized to the weighted average in the region $R_{jj} < 0.4$. In the large mass fraction region ($R_{jj} > 0.6$) a significant “dip” is observed in the data, indicating a contribution due to exclusive production (Fig. 4, center). The result is compared with the ratio of the inclusive dijets, where F_2 is the ratio of the inclusive MC events to the data (Fig. 4, right).

5. Exclusive photon pair production

Another process which can be used as “standard candle” is exclusive diphoton events, $p\bar{p} \rightarrow p\gamma\gamma\bar{p}$. The final state is cleaner than in exclusive dijet production as hadronization effects are absent, but the expected cross section is smaller. CDF has performed a search in this channel by requiring nothing else^a except two electromagnetic (EM) calorimeter towers above threshold in the final selection. Three exclusive $\gamma\gamma$ candidate events with $E_T > 5$ GeV are found with no tracks pointing at the clusters, with a small expected background. The purely QED $p\bar{p} \rightarrow pe^+e^-\bar{p}$ process is mediated through $\gamma\gamma \rightarrow e^+e^-$ scattering and constitutes a good control sample: 16 exclusive e^+e^- candidate events are selected in the data with a small background of $2.1^{+0.7}_{-0.3}$ events. The cross sections measured, $\sigma(\gamma\gamma) = 0.14^{+0.14}_{-0.04}(\text{stat}) \pm 0.03(\text{syst})$ pb and $\sigma(e^+e^-) = 1.6^{+0.5}_{-0.3}(\text{stat}) \pm 0.3(\text{syst})$ pb, are in agreement with expectations from exclusive ExHuMe and QED LPAIR MCs, respectively.

References

1. K. Goulianatos, hep-ph/0510035.
2. See, for example, B. Cox, AIP Conf. Proc. **792**, 540 (2005).
3. M. Gallinaro, “Prospects for Diffractive Physics with the CDF Forward Detectors at the Tevatron”, hep-ph/0407255; Presented at “Diffraction at the LHC”, Rio de Janeiro, Brazil, March 31-April 2, 2004, and references therein.
4. For each event, x_{Bj} is evaluated from the E_T and η of the jets using the equation $x_{Bj} = \frac{1}{\sqrt{s}} \sum_{i=1}^3 E_T^i e^{-\eta^i}$.
5. A. Affolder *et al.* [CDF Collaboration], Phys. Rev. Lett. **84**, 5043 (2000).
6. V. Khoze, A. Kaidalov, A. Martin, M. Ryskin and W. Stirling, hep-ph/0507040, and references therein.
7. B. Cox, J. Forshaw, Comput. Phys. Commun. **144**, 104 (2002). POMWIG implements the diffractive collisions, using all hard sub-processes, into the HERWIG Monte Carlo generator.
8. M. Boonekamp and T. Kucs, Comput. Phys. Commun. **167**, 217 (2005); DPEMC extends the POMWIG Monte Carlo generator to include new models of central production through inclusive and exclusive Double Pomeron Exchange in hadron collisions.
9. J. Monk and A. Pilkington, hep-ph/0502077; ExHuME implements the perturbative QCD calculation of Khoze, Martin and Ryskin of the process $pp \rightarrow pXp$, where X is a centrally produced colour singlet system.

^aIn this search, the leading hadrons are not detected.